Journal of Chromatography A, 1228 (2012) 193–204

Contents lists available at SciVerse ScienceDirect

Journal of Chromatography A

journal homepage: www.elsevier.com/locate/chroma

Review

Recent advances of mesoporous materials in sample preparation

Liang Zhao, Hongqiang Qin, Ren'an Wu*, Hanfa Zou**

National Chromatographic R&A Center, CAS Key Laboratory of Separation of Science for Analytical Chemistry, Dalian Institute of Chemical Physics, Chinese Academy of Sciences, Dalian 116023, China

ARTICLE INFO

Article history:
Available online 22 September 2011

Keywords:
Review
Advance
Mesoporous material
Sample preparation
Enrichment

ABSTRACT

Sample preparation has been playing an important role in the analysis of complex samples. Mesoporous materials as the promising adsorbents have gained increasing research interest in sample preparation due to their desirable characteristics of high surface area, large pore volume, tunable mesoporous channels with well defined pore-size distribution, controllable wall composition, as well as modifiable surface properties. The aim of this paper is to review the recent advances of mesoporous materials in sample preparation with emphases on extraction of metal ions, adsorption of organic compounds, size selective enrichment of peptides/proteins, specific capture of post-translational peptides/proteins and enzymatic reactor for protein digestion.

© 2011 Elsevier B.V. All rights reserved.

Contents

1. Introduction

In spite of the rapid development of various technologies in analytical chemistry, sample preparation is still a crucial step to achieve higher sensitivity and/or better specificity for the analysis of various analytes, especially for complex sample and trace level analytes [1]. Recently, mesoporous materials are gaining increasing research interest in sample preparation because of their desirable characteristics such as high surface area, large pore volume, tunable mesoporous channels with well defined pore-size distribution, controllable wall composition as well as modifiable surface properties.

According to the nomenclature by International Union of Pure and Applied Chemistry (IUPAC), porous materials can be classified into three categories: microporous material with pore size below 2 nm, macroporous material with pore size above 50 nm, and the mesoporous material with pore size between 2 and 50 nm. Due to the distinct mesopore structure, mesoporous materials have demonstrated their unique advantages in sample preparation: (1) mesoporous materials have highly ordered and size-controlled mesoporous structures which enable the size-selective adsorption of small molecules but the size-exclusion of larger molecules, providing the molecular weight cutoff in sample enrichment. For instance, the size-selective enrichment of endogenous serum peptides could be achieved by mesoporous materials due to the size-exclusion of mesoporous structure against the larger proteins in serum [2]. Though microporous material can also provide size selectivity for guest molecules, the main drawback is the limitation of mass diffusion [3]; (2) mesoporous materials have extremely

* Corresponding author. Tel.: +86 411 84379828; fax: +86 411 84379617.
** Corresponding author. Tel.: +86 411 84379610; fax: +86 411 84379620.
E-mail addresses: wurenan@dicp.ac.cn (R. Wu), hanfazou@dicp.ac.cn (H. Zou).

0021-9673/$ – see front matter © 2011 Elsevier B.V. All rights reserved.
doi:10.1016/j.chroma.2011.09.051

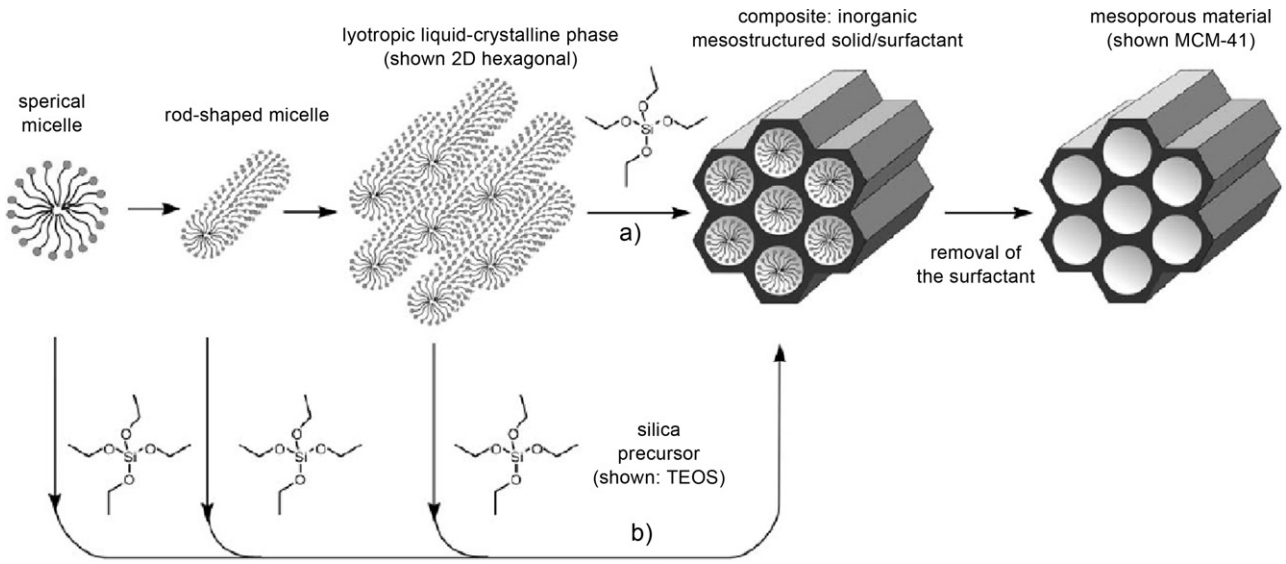

Fig. 1. Formation of mesoporous materials by structure-directing agents: (a) true liquid-crystal templating mechanism, (b) cooperative self-assembly process [17].

high surface areas and large pore volumes which provide the sufficient capacity for the adsorption of analytes; (3) mesoporous materials possess the performances in thermal stability, chemical stability, compositional controllability, and as well as the flexibility in post-functionalization to enable the further introduction of hydrophilic, hydrophobic, polar as well as positive or negative charged functional moieties on surface.

This work aims to review the general synthesis routes of mesoporous materials (especially silica, organic-silica hybrid, non-siliceous inorganic mesoporous materials and mesoporous carbon materials), and the recent achievements of mesoporous materials in sample preparation with emphasis on the extraction of metal ions, adsorption of organic compounds, enzymatic reactor for protein digestion and selective enrichment of peptides and proteins.

2. Synthesis of mesoporous materials

The scheme of the preparation of mesoporous material is illustrated in Fig. 1, which includes two routes to synthesize the mesoporous materials. The route a represents a true liquid-crystal templating procedure, which was first proposed by Mobil's scientists. Because the hydrophobic tails of templating surfactants are insoluble in polar solvents (i.e. water) while hydrophilic heads would tend to contact with polar solvents, the surfactants can thus self-assembly into micellar liquid crystals at concentrations greater than the "critical micelle concentrations" under certain temperatures. The formed surfactant micelle crystals then serve as the templates for the further formation of inorganic–organic composites around these crystals afterward the addition and subsequent condensation of silica precursors in solution. The route b represents another procedure of so called cooperative self-assembly process to the synthesis of silica mesoporous materials. In route b, the silica precursor and templating surfactant are first mixed, and then the surface of micelles in the silica precursor environment are evolved from sphere to rod and cluster driven by noncovalent weak interactions including hydrogen bonding, *van der Waals* forces and electrostatic attraction; via continuous polymerization and condensation of silica precursors, the ordered mesostructured inorganic–organic composites are finally formed. After the removal of surfactant templates by solvent extraction or calcination, the mesoporous materials with ordered mesochannels can be obtained. The structure and phase behavior of these mesostructured inorganic–organic composites depend on the nature of surfactant molecules and silica precursors. By selecting different types of surfactants (neutral block copolymer, cationic surfactants and anionic surfactants), additives (trimethylbenzene, alcohols and salt), synthesis temperatures, and basic or acidic reaction media, various silica mesoporous materials such as MCM-41 with two-dimensional hexagonal (*p6mm*) [4], SBA-12 with three-dimensional hexagonal ($P6_3/mmc$) [5], SBA-16 with three-dimensional cubic (*Im3m*) [6], lamellar [7], cellular foam [8] can thus be prepared with different pore structures. Besides the adjustment of mesoporous structure, mesoporous materials with different morphologies (thin films [9], fibers [10], particles [11], monoliths [12]) can be obtained by controlling the process conditions or parameters. Up to now, mesoporous silica materials with diverse compositions have been successfully synthesized. Here, the silica-based mesoporous materials employed in sample preparation are outlined in Table 1 [4,6,8,13–17] with their characteristic properties.

Organic-silica hybrid mesoporous materials have attracted the increasing research interest with the advantages of

Table 1
A summary of the characteristics properties of various silica mesoporous materials employed for sample preparation.

Mesoporous materials	Precursors	Template	Space group	Pore size (nm)	Refs.
MCM-41	TEOS, sodium silicate	CTAB, C_nTMA^+ (n = 12–18)	*p6mm*	2–10	[4]
SBA-16	TEOS, TMOS	F127, F108, or F98	*Im3m*	5–30	[6]
MCF	TEOS	F127 with TMB	*Cellular foam*	10–50	[8]
MCM-48	TEOS, sodium silicate	CTAB, C_nTMA^+ (n = 14–18), $C_{16}H_{33}(CH_3)_2N(CH_2C_6H_5)$	*Ia3d*	2–4	[13]
SBA-15	TEOS, sodium silicate	B50-1500 ($B0_{10}EO_{16}$), P123, P85, P65, Brij97($C_{18}H_{35}EO_{10}$)	*p6mm*	5–30	[14]
HMS	TEOS	$C_mH_{2m+1}NH_2$ (m = 8–22)	*wormlike*	2–10	[15]
FDU-12	TEOS	F127 ($EO_{106}PO_{70}EO_{106}$)	*Fm3m*	4–27	[16]
PMOs	$(RO)_3Si\text{-}R'\text{-}Si(OR)_3$	CTAB, OTAB, CPB, P123, F127, Brij56, Brij76	*Fm3m*, *Im3m*, *p6mm*	2–15	[17]

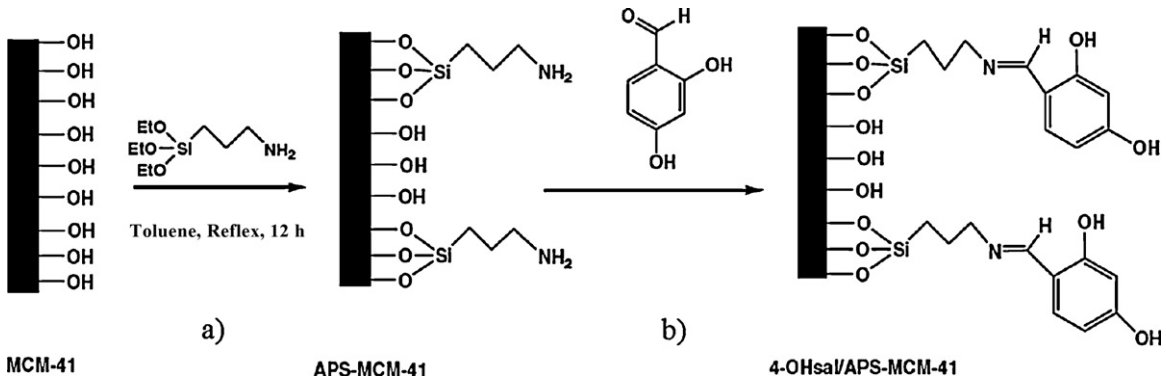

Fig. 2. Synthetic scheme: (a) preparation of (3-aminopropyl) triethoxysilane (APS)-MCM-41 and (b) preparation of 2,4-dihydroxybenzaldehyde (4-OHsal)/APS-MCM-41 [29].

compositing functional organic groups in silica. There are three major approaches to incorporate organic moieties into silica substrates [17]: (i) grafting organic groups onto pore surface using organosilanes, (ii) co-condensation of silica precursors and organosilanes, (iii) condensations of organic bridged silylated precursors. Via the aforementioned approaches, organic groups such as C–C multiple bonds, thiols, sulfonic and carboxylic acids, cyano, amine or aromatic groups have been incorporated into mesoporous materials [17,18]. Due to improved mechanical performance and thermal stability, the hybrid mesoporous materials should be promising in sample preparation.

Rather than the silica-based mesoporous materials, non-siliceous inorganic mesoporous materials (such as metal oxides and pure metal) and mesoporous carbon materials have also been applied in separation science. There are usually two approaches to synthesize these materials. One is self-assembling approach using soft-templates, similar to the synthesis of silica based materials, inorganic precursors (metal alkoxides or chlorides, carbon precursors) are usually used for self-assembly with amphiphilic block copolymer templates via chemical interactions including electrostatic attraction, hydrogen bonding, and hydrophobic/hydrophilic interactions [19]; another is using nanocasting strategy that takes highly ordered silica mesoporous materials (such as SBA-15, MCM-48) as 'hard template' and the inorganic precursors as the filling agents to fill up the mesochannels of 'hard template' to cast the mesostructured non-siliceous inorganic materials. Various non-siliceous inorganic mesoporous materials including ZrO_2, TiO_2, HfO_2, Gr_2O_3, Au, Pd, CMK-1 and CMK-3 have been successfully prepared by these methods [18,20–22].

Since extensive expatiations on the development of mesoporous materials have been reviewed elsewhere [17–20,23], we hereafter discuss the application of mesoporous materials with emphasis on sample preparation.

3. Application of mesoporous materials in sample preparation

3.1. Extraction of metal ions

Hazardous metals can get into food chains through various pathways with the consequence of causing fatal diseases as the accumulated metal ions in organs up to their certain limitations [24]. Various technologies have been developed for the determination of hazardous metals in polluted area, such as the spectrophotometry [25], electrochemical analysis [26], atomic adsorption spectrometry (AAS) [27], electrothermal vaporization inductively coupled plasma mass spectrometry (ETV-ICP-MS) [28], inductively coupled plasma optical emission spectrometry/mass spectrometry (ICP-OES/MS) [29,30], and inductively coupled plasma atomic emission spectrometer (ICP-AES) [31]. However, due to the complexity of sample matrix and the trace level of target metal ion in sample, it is often difficult to determine metal ions by these techniques directly. The effective extraction of hazardous metal ions from complex sample matrices is thus necessary. The solid phase extraction (SPE) is a widely applied technique with advantages of fast and simple operation, high enrichment performance, easy automation, cost effective etc. The distinctive characteristics of mesoporous materials (large surface area and pore volume) makes ordered mesoporous materials the ideal adsorbents for SPE.

2,4-Dihydroxybenzaldehyde functionalized mesoporous silica (MCM-41) has been applied as an adsorbent for the extraction of beryllium ion (Be^{2+}) from aqueous solution, followed by the detection of ICP-OES (as shown in Fig. 2) [29]. Under the optimized condition, the functionalized MCM-41 performed as a bidentate univalent anionic ligand to form chelate complex with Be^{2+}. This functionalized MCM-41 adsorbent had the ability to selectively enrich Be^{2+} from a mixed metal ion solution containing interferential metal ions of Cu^{2+}, Zn^{2+}, Co^{3+} with their concentrations 10,000 times higher than that of Be^{2+}. The maximum adsorption capacity of 34 mg g^{-1} could be achieved with a good reusability. Compared to other preconcentration methods (such as conventional SPE, precipitation and micelle-mediated), the method of using mesoporous materials demonstrated much lower LOD (0.3 ng L^{-1}). Besides, a variety of organic function groups have been introduced on the surface of mesoporous materials for the capture of different metal ions. Ordered mesoporous Al_2O_3 materials or mesoporous titanium film have also been used as capillary microextraction coating for the preconcentration of trace metal ions. Table 2 summarizes the preconcentration of metal ions by various functionalized mesoporous materials [26,30,32–38].

In addition, the ionic imprinting technique is an effective approach for the selective extraction of target analytes, which can generate plenty of specific recognition sites on mesoporous polymer materials via polymerization of cross-linking and functional monomers in the presence of the target analyte. For instance, Hoai et al. [39] has prepared copper (II) ion-imprinted mesoporous polymer materials for the extraction of Cu (II) ions. The results showed that the Cu (II) imprinted material had a higher affinity to copper ion rather than other metal ions, such as Ni, Zn. In comparison with commercial materials, the copper (II) ion-imprinted mesoporous polymer material demonstrated at least 10 times higher selectivity.

3.2. Adsorption of organic compounds

Volatile organic compounds (VOCs) are carbon-based chemicals in atmospheric environments. Many VOCs are demonstrated to be either toxic or even carcinogenic [40]. Since the concentrations of

Table 2
A summary of the functionalized mesoporous materials employed for preconcentration of metal ion.

Mesoporous materials	Functional groups	Metal ion	Adsorption capacity	Detection limit	Detection methods	Refs.
Mesoporous silica	Tetraacetamide derivative of cyclam	Pb^{2+}		2.7×10^{-9} M	Electroanalysis	[26]
Mesoporous silica	3-Aminopropyl	Cr^{5+}	4.35 mmol g^{-1}	1.2 pg mL^{-1}	AAS	[27]
Mesoporous TiO_2		V, Cr and Cu		1.1–6.3 pg mL^{-1}	ETV-ICP-MS	[28]
MCM-41	2,4-Dihydroxybenzaldehyde	Be^{2+}	34 mg g^{-1}	0.3 pg mL^{-1}	ICP-OES	[29]
Mesoporous Al_2O_3		As^{3+}, Cr^{3+}, As^{5+}, Cr^{5+}		0.7–74 pg mL^{-1}	ICP-MS	[30]
MCM-41	Thiophene-2-carbaldehyde	Pd^{2+}	5.0 mg g^{-1}	0.2 ng mL^{-1}	ICP-AES	[31]
SBA-15	5-Mercapto-1-methyltetrazole	Zn^{2+}	0.96 ± 0.01 mmol g^{-1}	8.0×10^{-9} M	FAAS	[32]
SBA-15	2-Mercaptopyrimidine	Cd^{2+}	0.99 ± 0.03 mmol g^{-1}		FAAS	[33]
Mesoporous silica	Chitosan	V, Cu, Pb, Cd and Hg	12.2–22.9 mg g^{-1}	0.05–0.96 ng mL^{-1}	ICP-OES	[34]
MCM-41	5-Nitro-2-furaldehyde	U^{5+}, Th^{4+}	47–49 mg g^{-1}	0.3 ng mL^{-1}	ICP-OES	[35]
Mesoporous TiO_2	Dimercaptosuccinic acid	As^{3+}, Sb^{3+}, As^{5+}, Sb^{5+}		0.10–0.15 ng mL^{-1}	ICP-OES	[36]
Mesoporous silica	3-(2-Aminoethylami-no) propyl	As^{3+},As^{5+}	10.3 mg g^{-1}	0.05 ng mL^{-1}	ICP-OES	[37]
SBA-15	Ethylenediamine	Cd^{2+}, Pb^{2+}	$360 \pm 1.4100.0 \pm 0.6$ mg g^{-1}		AAS	[38]

VOCs in air are at ppb or sub-ppb (v/v) levels, which are usually under the detection limits of modern gas chromatography (GC) based methods, the pre-concentration is generally of a necessary step to match the detection limits of applied analytical instruments. Based on hydrophobic interaction, a mesoporous material (MCM-41) with the pore size of 2.9 nm was applied in the in-line enrichment of VOCs (using C_2–C_{12} as a standard gas mixture) for gas chromatography coupled with flame ionization detection [41]. Compared to commercial available carbon molecular sieves (carbon adsorbents) for capturing C_3–C_{12}, MCM-41 material exhibits comparable adsorption ability for C_8–C_{12} other than for the highly volatile smaller compounds (C_3–C_7). In addition, the MCM-41 depicts the lower minimum desorption temperature (150 °C) as compared to that of carbon adsorbents (300 °C). By adjusting the temperature to sub-ambient temperatures (−20 °C), a full range of VOCs from C_4–C_{12} could be efficiently trapped by MCM-48 with pore size of 3.7 nm at a higher recovery. The highly efficient adsorption of VOCs at sub-ambient temperatures, the lower desorption temperature as well as the low memory effect have made mesoporous materials the promising in-line enrichment media for VOCs analysis by gas chromatography [42].

Powdered activated carbons (ACs) with an important mesoporous volume and distinct surface chemistry characteristics are used as adsorbent phases to purify triazinic herbicides (atrazine, simazine and terbutylazine) in environmental water matrices, followed by liquid desorption and high performance liquid chromatography with diode array detection [43]. Under optimized conditions (extraction time, pH, ionic strength), recovery around 100%, detection limits about 0.1 μg L^{-1}, and suitable linearity (1.0–12.0 μg L^{-1}) have been achieved. This proposed methodology has been proved to be a suitable way to monitor traces levels of these three herbicides in water matrices.

Likewise the molecular imprinting technology for the preparation of the molecularly imprinted polymers (MIPs), a surface imprinting method has also been applied in the synthesis of mesoporous material for the selective analysis of target analytes. As shown in Fig. 3, some organic moieties can be incorporated into the skeleton of mesoporous material via the organic–inorganic hybrid sol–gel process by using the certain organic groups bridged silsesquioxanes. Because of the molecular affinity of the organic moieties on the skeleton of organic–inorganic hybrid mesoporous materials, these surface imprinted mesoporous materials have demonstrated the enhanced selectivity and sensitivity to the target analytes, which are analogous to the imprinted organic moieties. Trammell et al. [44] realized the use of nanoporous organosilicas for the rapid preconcentration and extraction of trinitrotoluene (TNT) for electrochemical analysis and demonstrate the effect of template-directed molecular imprinting on TNT adsorption. They developed two types of TNT imprinted nanoporous organosilicas for the preconcentration of TNT prior to electrochemical analysis. One is benzene (BENZ)-imprinted hybrid organic–inorganic having high BET surface area (980 m^2/g) and large pore volume (0.714 cm^3/g) with highly ordered mesopore structure; another is the diethylbenzene (DEB)-imprinted hybrid organic–inorganic one possessing amorphous pore structure with BET surface area of 35 m^2/g and small pore volume of 0.0331 cm^3/g. In a comparison, the DEB-imprinted material was 7 times more efficient than the nonimprinted one in the capture of TNT from aqueous contaminated soil samples. In addition, the limit of detection of the BENZ-bridged mesoporous materials (30 ppb) is much lower than that of the DEB-bridged adsorbents (90 ppb) in the enrichment of TNT from 500 μL sample. This surface imprinting technique could be adopted to analyze other target analytes of interest by using corresponding organic compounds (diethylbenzene, porphyrins analog) as bridge moiety in the synthesis of hybrid inorganic–organic mesoporous materials [45,46].

Spherical chiral mesoporous polypyrrole (CMPPy) nanoparticles have been synthesized by incorporating chirality into the mesochannels and applied to recognize chiral molecules, which are detected by circular dichroism and optical polarimetry [47]. With the three dimensional imprinted chiral mesostructures, CMPPy nanoparticles display remarkable chiral selectivity and selective adsorption in the mesochannels. Using these chiral nanoparticles,

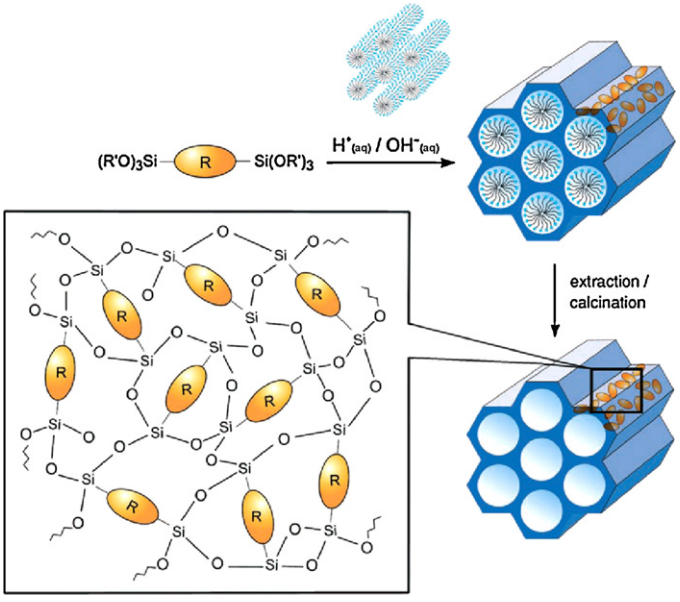

Fig. 3. General synthetic pathway to surface imprinted hybrid mesoporous materials that are constructed from bissilylated organic bridging units. R = organic bridge, which has affinity for the analytes analog to the organic moieties [17].

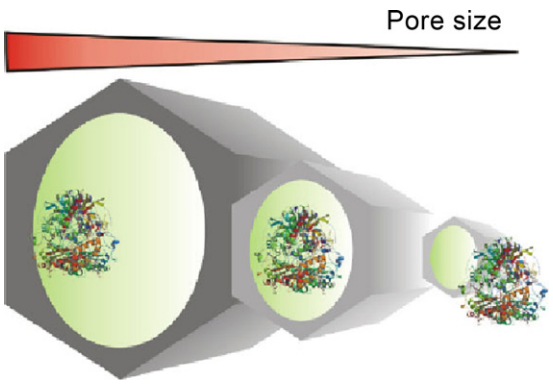

Fig. 4. Diagram of protein adsorption in mesoporous materials with different pore sizes: the matched pore size (middle); while, the larger pore size (left) or smaller one (right) [48].

pure chiral molecules (L-valine) from a racemic mixture could be stereoselectively recognized and separated. In this way, various chiral materials can be synthesized in this simple, controllable and cost effective way.

3.3. Enzymatic reactor for protein digestion

Proteomics have attracted much attention in recent years because of its ability to elucidate the key roles of proteins in biological process and discover potential biomarkers [1,47]. The "shot-gun" proteomics requires protein digestion (in most cases by trypsin) before mass spectrometry analysis. The conventional enzymatic digestion is in free solution, which often suffers from the serious interference of the autodigestion of enzymes. Protein digestion by the immobilized enzyme has been considered a promising enzymatic digestion technology due to the advantages in enzyme stability, digestion efficiency, enzyme recycling and free of product contamination.

For enzyme reactor, it is important to choose the proper pore size and spatial structures, as well as the surface properties including hydrophilicity, hydrophobicity, charge status, different organic groups etc, since these factors may affect the activity and stability of included enzyme. As shown in Fig. 4 [48], if the pore size is smaller than the dimensions of enzyme, the enzyme would adsorb onto the external surface, resulting in low stability and low adsorption capacity; when the pore size of mesoporous is sufficiently larger for the entrapment of biomolecules, enzyme would penetrate into the mesochannels rather than adsorb onto the outer surface. If enzymes were reversibly immobilized by weak physical adsorptions, such as hydrogen bonding, hydrophobic attraction or electrostatic interaction, the adsorbed enzymes would leach out the mesoporous channels. By covalently binding enzymes on reactive groups such as aldehyde, epoxide and thiol groups, or by cross-linking the enzymes inside the mesoporous channels, the immobilization stability could be greatly enhanced and the covalent or cross-linked enzymes can be recycled for the repeat usage. Hyeon et al. reported that the immobilized trypsin remained its 89% initial activity in mesoporous materials by cross-linking with glutaraldehyde even after 29 iterative cycles of enzyme reaction [49]. Besides, the balance of the hydrophobic and hydrophilic interaction between enzyme and material is also known to impact the stability and activity of immobilized enzyme [48,50]. Rotello et al. reported that the denaturation extent of chymotrypsin could be considerably reduced by introducing of hydrophilic ethylene glycol as space arm between the surface and the immobilized enzyme [51,52].

To achieve the rapid digestion, large sequence coverage and high sensitivity for broad range proteins with diverse physical properties, Shui et al. [53] developed a novel proteolytic nanoreactor using a mesoporous silica of FDU-12 with a unique three-dimensional nanopore structure. This nanoreactor integrated substrate enrichment, "reagent-free" protein denaturation, and efficient proteolytic digestion in the mesoporous space of FDU-12. In this design, protein substrates were first captured by the mesoporous material of FDU-12 and then were concentrated from solution. Following by pH change and applying trypsin, the denaturation and concurrent proteolysis of broad-range proteins could be efficiently achieved, resulting in the identifications of a broad range of diverse proteins with high sequence coverage by mass spectrometry. Similarly, trypsin immobilization on SBA-15 or amine and cyano functionalized SBA-15 materials have also been applied for protein proteolysis [54–56]. Casadonte et al. [54] found that the amine functionalized SBA-15 showed higher digestion efficiency than unmodified SBA-15 with the same pore diameters. Also, the proteolytic efficiency of functionalized SBA-15 was 1000 times faster than that of using conventional free solution method. Interestingly, the digestion performance could be enhanced by increasing the length of the amine group, which seemed to attribute to the stabilization effect of the longer amine group to enzyme. Though the adsorption of enzyme on material via electrostatic interaction is simple, the risk of enzyme leaching out is still a concern.

The analysis of low-molecular-weight (LMW) proteins is often very difficult, because the separation of LMW proteins from complex protein sample by various separation techniques is time consuming and would resulted in sample loss. Recently, a size-selective digestion of LMW proteins was developed by using a mesoporous silica material [57]. As shown in Fig. 5, trypsin was covalently immobilized on the thiol-modified SBA-15 material and confined in mesochannels of SBA-15 with the pore size of ca. 5.7 nm. Due to the size-exclusion interaction of mesopores of the thiol-modified SBA-15 material to the big size protein of BSA ($5.0 \times 7.0 \times 7.0\,nm^3$), the material could exclude high-molecular-weight (HMW) protein of BSA but capture LMW proteins (<5.7 nm) of cytochrome C, lysozyme, myoglobin for giving the chance to carry out the enzymatic digestion by the immobilized trypsin. By this size-selective digestion, the LMW proteins could be selectively digested by the immobilized trypsin but not the HMW proteins.

3.4. Size-selective enrichment of endogenous peptides and proteins

Peptidomics, referring to all of LMW peptides or proteins, is defined as the systematic analysis of endogenous peptides and small proteins in biological sample (such as body fluids, cell lysate, and tissue extract) at a defined time points and/or locations [58–60]. Peptides from these biological samples may have the potential to serve as biomarkers, indicating of progression from a normal to a diseased status [61]. Thus, peptidomics based on mass spectrometry technology has been established and emerged as a promising strategy to characterize the native peptides or small proteins, resulting in comprehensive understanding of native peptides/proteins in biological processes. However, due to the complexity and high dynamic range of endogenous peptides and the interference from high concentrations of proteins, salts and lipids in biological samples, the ability to extract peptides/small proteins from the complex biological samples as well as enhancing the sensitivity toward peptides/small proteins at low abundance, remains a great challenging task before MS analysis. Thus, various methods (ultrafiltration [62], solid-phases extraction [63], selective electrophoresis and continuous elution electrophoresis [64], organic solvent precipitation [65]) have been developed to isolate peptides/small proteins before MS analysis. Centrifugal ultrafiltration with accurate MW cutoff is one widely used method for peptide enrichment based on size-exclusion effect. Unfortunately, it would take a long time to operate and co-concentrate some small

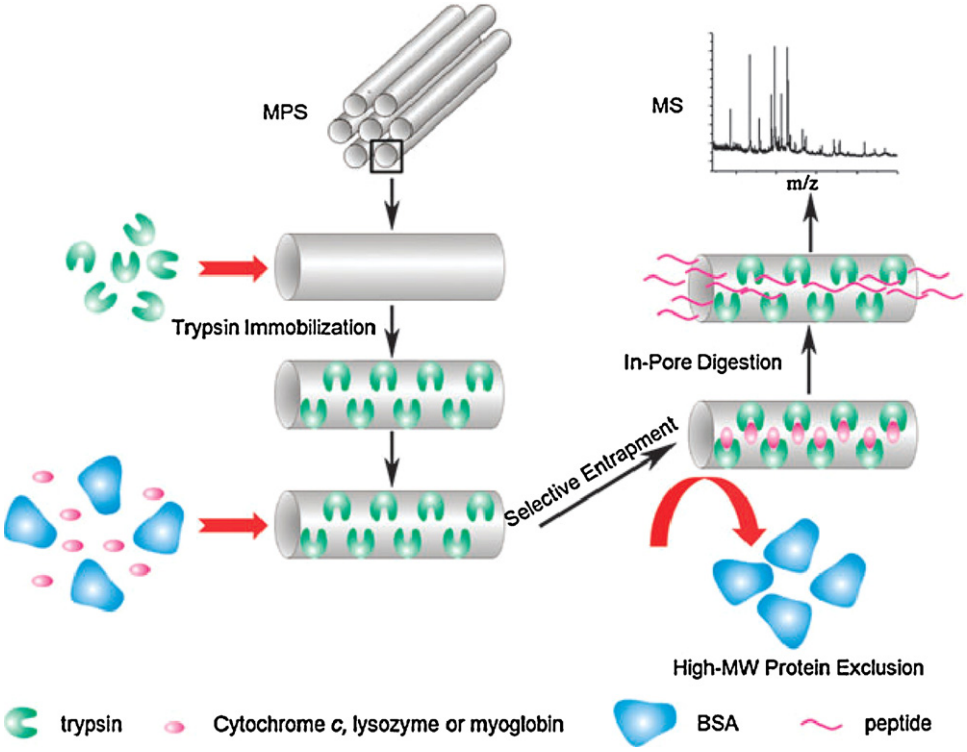

Fig. 5. Schematic procedure of size-selective proteolysis of small proteins (Cyt c, lysozyme or myoglobin) from a high-molecular-weight protein (BSA) [57].

molecule contaminants (such as salt) if a huge amount of biological sample is applied, resulting in low enrichment efficiency, which limited its practical application [62].

Mesoporous materials are attractive candidates for the enrichment of peptides. The efficiency of size-dependent separation based on mesoporous materials is determined by the relation of pore size to the diameter of target molecules. Biomolecules whose sizes are smaller than the pore size of mesoporous material can be captured in the pore channel, while biomolecules larger than the pore size are excluded by the pore channel. Besides the size effect, hydrophobic and electrostatic interactions between peptides/proteins and materials along with other factors including 3D hydrodynamic dimensions of the protein, hydrogen bonding with water may also affect the adsorption of biomolecules on mesoporous materials [66].

Various functionalized mesoporous materials have been developed for the enrichment of peptides from biological samples. Recently, Tian et al. [2] developed highly ordered mesoporous materials possessing different pore size (2, 8, 12 nm) to adsorb standard protein lysozyme, and found MCM-41 with the pore size of 2 nm could be used to selectively and effectively enrich low-molecular-weight peptides/proteins from human plasma with a cutoff of 12 kDa, based on the combined effect of hydrophobic and size-exclusion interactions. The typical MALDI-TOF MS results are shown in Fig. 6. The unique property of mesoporous material made it superior adsorbent for enrichment of peptides or small proteins. To improve the enrichment efficiency and capacity, Tian et al. [60] further synthesized different functionalized MCM-41 with strong cation-exchange and strong anion-exchange properties. As shown in Fig. 7, by combination of anion-exchange, cation-exchange and hydrophobic mechanisms, endogenous peptides from mouse liver extract were selectively enriched and consequently analyzed by 2D nano-LC/MS/MS. Because the hydrophobic interaction between peptides and mesoporous materials can be enhanced by introducing organic groups ($-CH_2-$) on the walls of mesoporous channels in the synthesis of periodic mesoporous organosilica (PMO) materials, Wan et al. [67] reported amino group (NH_2) functionalized PMO materials (NH_2-PMO) with an organo-bridged ($-CH_2-$) hybrid wall composition. Due to the charge status, PMO (-25.2 mV) and NH_2-PMO (+39.0 mV) can enrich positively charged and negatively charged peptides, respectively. As a result, 69.4% (25 of 36) of peptides with $pI \geq 6$ were enriched by PMO and 80% (21 of 28) of peptides with $pI \leq 6$ were captured by NH_2-PMO. Thus, more comprehensive and complementary information can be collected by combination of these two types of functionalized PMO materials.

Hu et al. [68] synthesized mesoporous silica (MPS) thin film with various pore size distribution, pore structure, and connectivity. The effect of the pore structure of mesoporous silica on the enrichment efficiency and specificity of low molecular-weight from human plasma was investigated. It was observed that because of the increased pore connectivity and the reduced steric hindrance, the mesoporous silica with 3D cubic nanostructure or 3D honeycomb hexagonal nanostructure exhibited superior performance in capture of LMW peptides than the MPS with 2D hexagonal nanostructure, in despite of similar pore size distribution and the same mass cutoff. Nevertheless, with the same 3D nanostructure of MPS, the recovery of LMW proteins would also be affected by pore size (3, 4, 6 and 7 nm) of MPS.

In order to facilitate the enrichment process, magnetic mesoporous silica mesoporous materials have been also developed for the magnetic separation. As shown in Fig. 8, Chen et al. [69] reported a facile and low-cost way to synthesize $Fe_3O_4@nSiO_2@mSiO_2$ microspheres, which were applied in the selective enrichment of low-concentration peptides. By combining the magnetic property and mesoporous silica shell structure, the process of peptide enrichment is convenient, fast and efficient, which has been demonstrated in the enrichment of endogenous peptides from rat brain extract based on the hydrophobic interaction between hydrophobic peptides and siloxane bridge groups on inner wall of mesoporous channels. Since the prepared $Fe_3O_4@nSiO_2@mSiO_2$ microspheres could only be used to capture hydrophobic peptides rather than hydrophilic peptides, Cu^{2+} functionalized magnetic

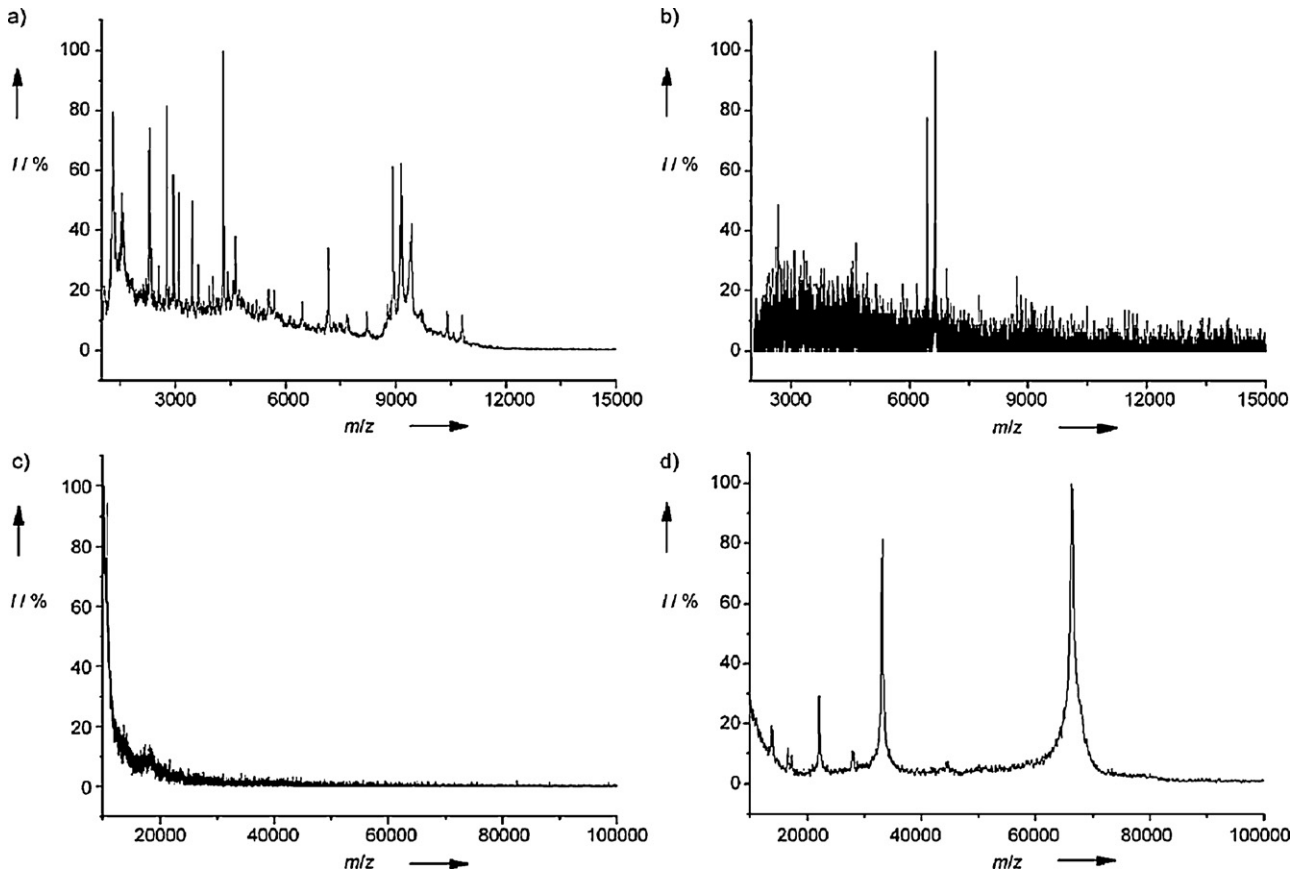

Fig. 6. MALDI-TOF MS analysis of human plasma (a, c) after and (b, d) before treated by MCM-41 with a-cyano-4-hydroxycinnamic acid as MALDI matrix. Analysis in the molecular-weight range of (a, b) 1–15 kDa and (c, d) 10–100 kDa [2].

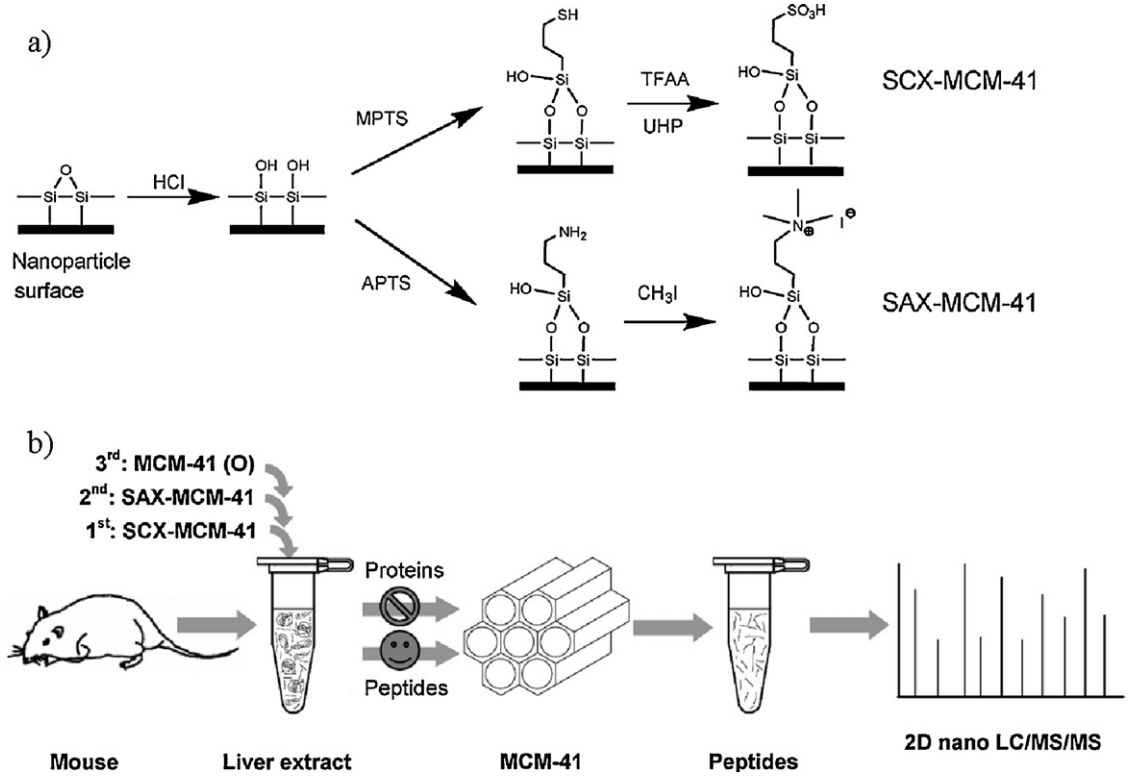

Fig. 7. Schematic overview of (a) the preparation of SCX-MCM-41 and SAX-MCM-41 materials; (b) the work flow for endogenous peptide enrichment and identification; the endogenous peptides from mouse liver are enriched by three kinds of mesoporous materials before analysis with 2D nano-LC/MS/MS [60].

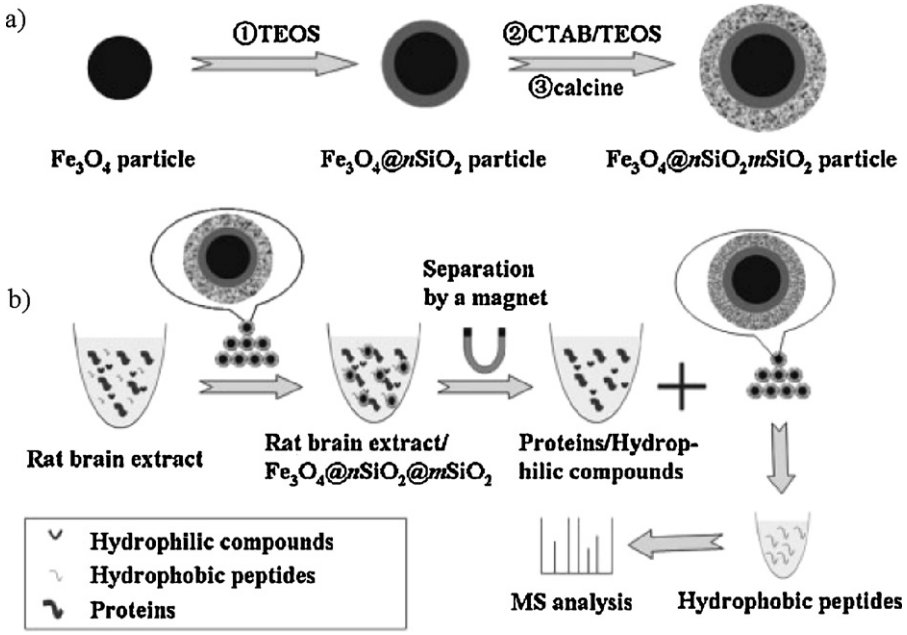

Fig. 8. (a) The synthesis route of $Fe_3O_4@nSiO_2@mSiO_2$ microspheres and (b) schematic illustration of fast and convenient enrichment protocol for endogenous peptide by using $Fe_3O_4@nSiO_2@mSiO_2$ microspheres [69].

mesoporous silica microspheres ($Fe_3O_4@mSiO_2$–Cu^{2+}) with magnetic core and mesoporous silica shell were developed for the enrichment of hydrophilic peptide via the immobilized metal ion affinity chromatography (IMAC) [70]. The enrichment mechanism is that the large amount of immobilized Cu^{2+} could interact with hydrophilic peptides via the coordination between copper (II) ion and carboxylic and amino groups of peptides.

By mimicking biological membrane, mesoporous materials are also used to size selective separation of biological macromolecules, such as proteins. The efficiency of size-based is dependent on the hydrodynamic diameter of proteins in a given electrolyte. It is reported that proteins can be passed through the mesoporous channels with the pore diameters as approximately three times larger than that of target proteins [71]. With the anodization process, Roy et al. [66] prepared a TiO_2 membrane with defined mesochannels (average pore size of 8-12 nm) for the size selective protein separation. Three proteins with different Stokes radii [cytochrome C (1.63 nm), BSA (3.62 nm) and β-galactosidase (6.86 nm)] are selected to evaluate the efficiency of size-dependent separation. It was found that cytochrome C and BSA could pass through the mesochannels while the large molecule β-galactosidase are excluded. Clogging of mesochannels is a sticky problem occurring in all size separation devices if the pore opening is in the size range of the smallest excluded proteins. Therefore, a main merit of these TiO_2 membranes is their photocatalytic activity, which is able to effective declogging of these membranes when applied to separate proteins. Mesoporous silica coated carbon nanotubes [72], mesoporous polymer coated copper hydroxide nanostrands [73], magnetic silica nanospheres with highly ordered periodic mesostructure [74] and lysozyme imprinted polymer beads [75] are also synthesized for the selective separation of proteins with different molecular sizes.

3.5. Specific capture of post-translational peptides and proteins

Protein phosphorylation is one of the most important post-translational modification involved in many biological processes, such as cellular growth, division and signaling [76,77]. Aberrant phosphorylation has been known to be related to underlying many human diseases, especially human cancer [78]. To achieve detailed understand on the reversible phosphorylation-controlled biological processes, it is therefore necessary to characterize the phosphorylated peptides and their sites. Mass spectrometry based methods has been proved to be a powerful tool for the analysis of phosphorylated peptides [79,80]. However, because of the low abundance of phosphorylated peptides, interference from excessive amounts of nonphosphorylated peptides and the low efficiency in ionization of negative charged phosphorylated peptides, it is still a great challenge on the large scale analysis of phosphorylated peptides. Therefore, it demands to effectively isolate and enrich phosphorylated peptides or proteins from biological samples prior to MS analysis.

One of the most widely employed methods to enrich phosphopeptides is affinity-based chromatography, which is divided into two categories. The first one is metal oxide affinity chromatography (MOAC) using titanium dioxide (TiO_2) [81], zirconium dioxide (ZrO_2) [82], and ferric oxide (Fe_2O_3) [83]; the second one is immobilized metal ion affinity chromatography (IMAC), which has chelating ligand (iminodiacetic acid (IDA) or nitrilotriacetic acid (NTA)) on chromatographic adsorbents for immobilizing metal ion (Fe^{3+} or Ga^{3+}) [84,85].

For MOAC, metal oxides display amphoteric properties based on unsatisfied valences. In acidic solution, metal oxides behave as a Lewis acid with positively charged metal ions, which can be preferentially and reversibly exchanged with negatively charged molecules (such as phosphate, carboxylate, sulfate groups); while in basic solutions, the negative charged molecules can be eluted from the adsorbents. Mesoporous metal oxides with well ordered porosity are stable over a wide pH range, and provide many active sites for binding phosphate groups, which may be translated into even larger binding capacity than micro or nano metal oxides. Thus, mesoporous metal oxides may have more superior performance in phosphoproteomics.

Tang et al. [86] reported that mesoporous TiO_2 microspheres were applied as potential MOAC adsorbents for purification of phosphopeptides. The surface area of mesoporous TiO_2 microspheres (84.98 m^2/g) with the diameter of about 1.0 μm is almost two times of commercial TiO_2 nanoparticles (a diameter of 90 nm)

and is much larger than that of smooth TiO_2 microspheres (3.35 m^2/g), so these superior properties provide mesoporous TiO_2 microspheres with greater binding capacity and higher capture efficiency than that of smooth TiO_2 microspheres and TiO_2 nanoparticles in phosphoproteome analysis. As an adsorbent for enrichment of phosphopeptides, Han et al. [83] found mesoporous Fe_2O_3 microspheres with an averaged inter-particle pore size of 48 nm can eliminate the shadow effect, because mesoporous of Fe_2O_3 microspheres are large enough to freely release trapped peptides (<2 nm) from the inner-pore surface to the outer surface under laser irradiation. Lu et al. [87] synthesized mesoporous TiO_2 nanocrystal clusters with modification of hydrophilic and negative outer surface, three dimensional pores, submicrometer size and high ratio of surface area to volume, making the clusters more dispersible in water solution and can enhance the adsorbent more accessible to the phosphopeptides, resulting in much larger binding capacity, higher selectivity and higher sensitivity than that of solid TiO_2 spheres using α or β-casein as model protein. Nelson et al. [88] first reported mesoporous ZrO_2 metal oxides showed higher specificity and efficiency for phosphopeptides than that of commercial IMAC and ZrO_2 nanoparticles packed tip, and then evaluated the performance among mesoporous TiO_2, HfO_2 and ZrO_2 metal oxides for enrichment of phosphopeptides from tryptic digests of α-casein in another report [89]. The results showed that the enrichment specificity (>99%) using mesoporous HfO_2 and ZrO_2 is fairly comparable, and is higher than that of using mesoporous TiO_2; moreover, mesoporous TiO_2 and HfO_2 tend to effectively enrich multiple phosphorylated peptides while mesoporous TiO_2, HfO_2 and ZrO_2 appeared to be similar affinity toward mono phosphorylated peptides in general; interestingly, mesoporous HfO_2 and ZrO_2 can be repeatedly used in the enrichment of phosphopeptides with comparable performance to that of freshly prepared materials after a simple solution regeneration procedure. Similarly, zirconium layer coated mesoporous silica microspheres (MCF) [90] or titanium layer coated magnetic hollow mesoporous silica microspheres [91] are also applied to enrich phosphopeptides from standard proteins.

However, sample loss during various steps of enrichment procedure (centrifugation or elution) is unavoidable. In order to reduce sample loss and facilitate the sample preparation in the enrichment procedure, on-target and magnetic enrichment strategies are also taken. MALDI plate was modified by mesoporous anatase TiO_2 and employed to analyze phosphopeptides [92], the enrichment is directly operated on the modified MALDI plate and the non-specifically peptides unbound to the plate can be easily removed with washing buffers. Using this strategy, mesoporous anatase TiO_2 spots can be able to enrich very low and substoichiometric amounts (≈3 fmol) of phosphopeptides; a thin stripe made of mesoporous TiO_2 sintered onto a conductive glass surface, which is analogous to thin layer chromatography, was used to enrich and separate multi- and monophosphorylated peptides [93]. Moreover, Fe_3O_4@SiO_2@$mCeO_2$ with a magnetic core and mesoporous shell have also been applied to simultaneously enrich and label phosphopeptides (dephosphorylation) due to its affinity and catalysis properties [94].

The mesoporous metal oxides have indeed shown strong application in efficient enrichment of phosphopeptides. However, large scale analysis of phosphopeptides may not be achieved by MOAC-based methods because of the presence of steric hindrance and also the not so well biocompatibility inorganic metal oxides.

IMAC is the most well-known affinity method in phosphoproteome analysis, which is based on strong specific interaction between metal ion on adsorbents and phosphate groups of phosphopeptides. However, conventional IMAC adsorbents are modified with IDA or NTA as ligands to immobilize Ga^{3+} or Fe^{3+}, and still lack enough specificity to phosphopeptides due to the significantly unselective co-enrichment of highly acidic peptides, which

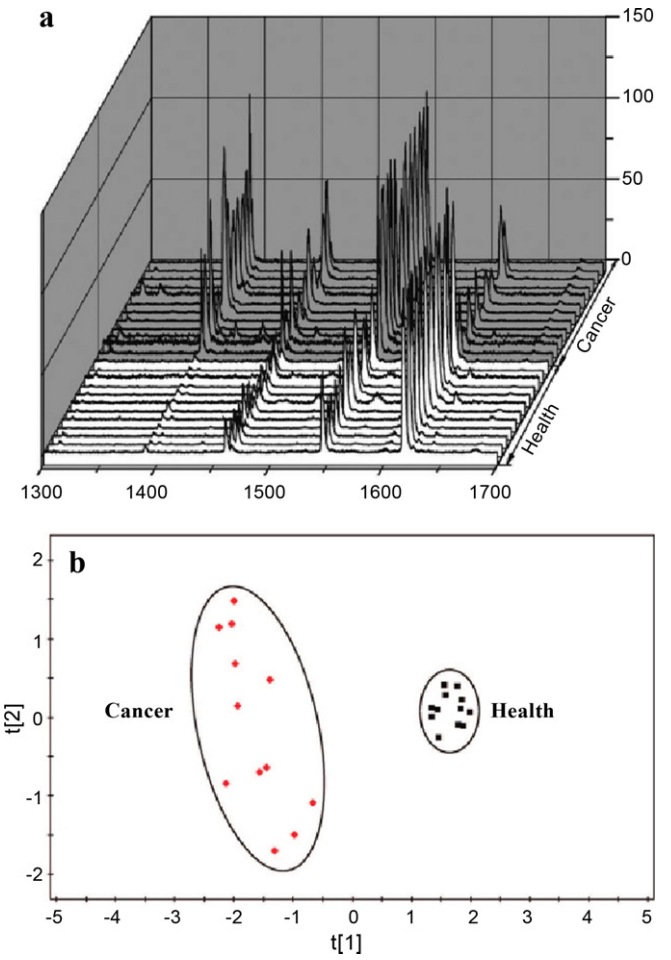

Fig. 9. (a) 3D view of the MALDI-TOF-MS profiling of phosphopeptides enriched from sera of hepatocellular carcinoma cancer (HCC) patients and healthy persons. (b) Partial least-squares discriminant analysis score plot showing the separation between the HCC cancer and healthy groups [96].

results in low selectivity and sensitivity for targeted phosphopeptides. In our lab, Fe^{3+} and Zr^{4+} phosphate functionalized periodic mesoporous organosilicas with ordered 2D hexagonal mesostructures, high specific surface area and large pore volume have been applied to enrich phosphopeptides, which showed higher intensities and signal/noise ratios of the enriched phosphopeptides than that of commercial POROS 20 loaded with the same metal ion [22]. Ti^{4+} incorporated hexagonal mesoporous silica (Ti-HMS) with relative high Ti-content (2 and 8 mol%) are successfully synthesized in our lab for the enrichment of phosphopeptides [95]. It was found that the Ti-HMS with higher content (8%) of titanium could effectively enrich three phosphopeptides from β-casein; while, Ti-HMS with lower content (2%) of titanium could only enrich one multiple phosphorylated peptides due to the relatively low content of titanium incorporated in the silica framework of Ti-HMS. Hu et al. [96] also synthesized titanium phosphate modified highly ordered mesoporous silica microparticles and applied to enrich phosphopeptides from β-casein as well as human serum. Because of high surface area, large pore volume and ordered mesoporous of the synthesized material, the detection limit for phosphopeptides enrichment from β-casein and standard phosphopeptide spiked human serum can be as low as 1.25 fmol analyzed by MALDI-TOF MS. Based on size-exclusion and adsorption effect by mesoporous silica particles, four endogenous phosphopeptides were effectively enriched from human serum. By combination of the direct use of MALDI profiling and isotope labeling, as shown in Fig. 9, it was

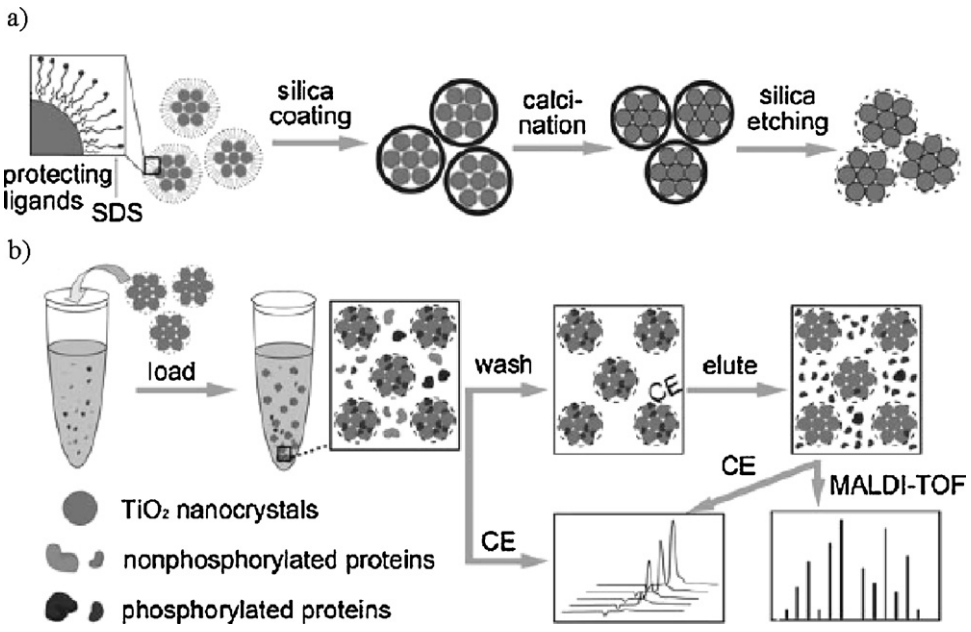

Fig. 10. Illustration of (a) the procedure for the fabrication of the mesoporous TiO_2 nanocrystal clusters and (b) the selective enrichment process of phosphorylated proteins using the mesoporous TiO_2 clusters and the elutes were analyzed by CE or MALDI-TOF MS [97].

found that four endogenous phosphopeptides were differentially expressed between cancer and health persons, thus making the developed approach as a potential biomarker discovery for clinical research. This approach is effective for the profiling of phosphopeptides in complex biological samples and the discovery of biomarker based on functional mesoporous materials.

The above reported techniques based on affinity chromatography are all used to enrich phosphopeptides at peptide level and indirectly provide information about phosphorylated protein. As shown in Fig. 10, Lu et al. [97] described the preparation self-assembled TiO_2 nanocrystal clusters with different averaged pore sizes of 2.3, 2.5 and 3.5 nm, and their application on selective enrichment of phosphorylated proteins from a mixed solution of three proteins (one phosphorylated β-casein, two non-phosphorylated horseradish peroxidase and β-lactoglobin). Only β-casein was detected by capillary electrophoresis with UV detection at 200 nm when using the mesoporous TiO_2 clusters. In comparison, TiO_2 solid spheres are failed to trap β-casein. These results indicated that trapping of phosphorylated protein not only depended on the affinity of TiO_2 but also the mesoscale pores.

Protein glycosylation is also a most common post-translational modification and plays very important role in cell communication, signaling and cell adhesion [98]. However, comprehensive studies on protein glycosylation have been complicated by the diverse structure of protein glycans. Though various strategies such as lectin affinity chromatography [99], hydrophilic interaction liquid chromatography [100], hydrazide chemistry [101] have been developed, a sensitive, quick and applicable method for enrichment of glycopeptides is still needed. As shown in Fig. 11, Xu et al. [102] synthesized a novel boronic acid functionalized mesoporous silica material (FDU-12-GA). Because of its prominent features of high surface area, large pore volume, and narrow distribution of regular pore size, a high percentage (up to 32 wt%) of grafted organics has been incorporated into the material. Glycopeptides with the recovery of 83.5% can be effectively and specifically enriched from complex tryptic peptide mixture in 15 min, while the commercial boronic acid functionalized magnetic beads would take 60 min; by

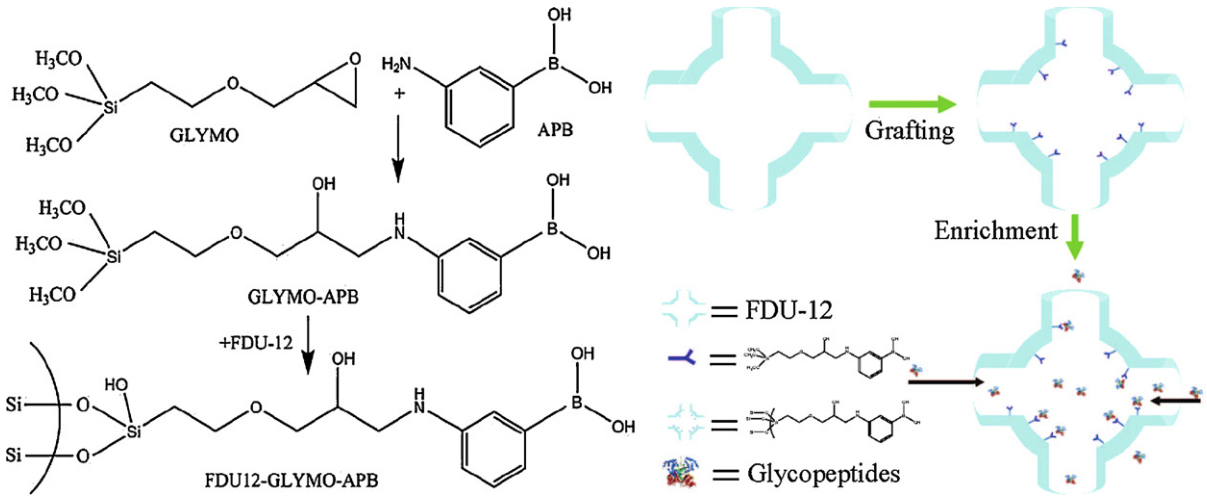

Fig. 11. Postsynthetic steps (left) of ordered mesoporous di-boronic acid functionalized FDU-12 (denoted as FDU-12-GA) [102].

the elimination of the suppression effect from nonglycopeptides, the limit of detection for glycopeptides is greatly enhanced by close to 2 orders of magnitude.

4. Conclusion

Mesoporous materials are promising adsorbents in sample preparation due to their distinct physicochemical properties in surface area and pore structure as well as the versatile availability in surface functionalization to provide the hydrophobic, hydrophilic, positively and negatively charged surface to interact with analytes. The combination of the size-exclusion effect of mesopores against big size molecules and the adsorption of small size analytes inside the mesopores actually mimics the effect of multidimensional chromatographic separation of integrating molecular filtration (by tunable highly ordered mesopore) and solid-phase extraction (by internal hydrophobic, hydrophilic, positively and negatively charged inner surface, etc.) of analytes on-beads, which can greatly simplify the sample preparation procedure by avoiding the multi-step filtration, washing, extraction and elution.

Although mesoporous materials have demonstrated unique advantages in sample preparation, some issues associated with their synthesis and application are yet to be resolved. First, the low stability of mesoporous silica materials under strong acid or basic conditions will inhibit their application as solid phase adsorbents at some extreme pH conditions. Second, the pore size distribution of mesoporous materials could not be exactly controlled as we designed. Third, post modification is an effective way to endow mesoporous materials with various functional groups, but this severe way only provides uneven functional groups on the external/internal surface and may decrease or even block the porosity. Organic groups can be homogeneously introduced to the surface of mesoporous materials, but the mesostructural ordering would be affected with the increase content of organosilanes or organic bridged silylated precursors, resulting in decrease of adsorption amount. Fourth, conventional synthesized mesoporous materials are usually very bulky, and the orientation of mesochannels run along the long axis, so the length of mesochannels is very long, it may take a long time to fully adsorb biomolecules, which would be not favorable for the quick analytical requirement. Thus, ideal mesoporous adsorbents should possess high density of functional groups, short and accessible mesoporosity, controllable morphology (such as 3D cubic nanostructure or 2D hexagonal nanostructure), fast molecular diffusion and adsorption kinetics. Yet, mesoporous metal oxides, carbon or polymer based mesoporous materials with different properties require in-depth studies in sample preparation, especially for biological samples such as glycans, peptides, lipids and other post-translational proteins. Furthermore, multifunctional mesoporous materials with magnetic, optical, electronic properties and tailored morphology (such as pore size, mesoporous structure, wall compositions, and surface properties) are also crucial factors in enhancement of selectivity and efficiency in sample preparation.

Acknowledgements

This work was supported by the National Natural Science Foundation of China (Nos. 20735004, 20875089), the Creative Research Group Project by NSFC (21021004), the State Key Basic Research Development Program of China (No. 2007CB914102), the National High Technology Research and Development Program of China (No. 2008AA02Z211), the Key Program of Knowledge Innovation (KSCX2-YW-G-049) and the Hundred Talent Program of the Chinese Academy of Sciences.

References

[1] N.L. Anderson, N.G. Anderson, Mol. Cell. Proteomics 1 (2002) 845.
[2] R. Tian, H. Zhang, M. Ye, X. Jiang, L. Hu, X. Li, X. Bao, H. Zou, Angew. Chem. Int. Ed. 46 (2007) 962.
[3] Y. Tao, H. Kanoh, L. Abrams, K. Kaneko, Chem. Rev. 106 (2006) 896.
[4] C.T. Kresge, M.E. Leonowicz, W.J. Roth, J.C. Vartuli, J.S. Beck, Nature 359 (1992) 710.
[5] Q.S. Huo, D.I. Margolese, G.D. Stucky, Chem. Mater. 8 (1996) 1147.
[6] D.Y. Zhao, Q.S. Huo, J.L. Feng, B.F. Chmelka, G.D. Stucky, J. Am. Chem. Soc. 120 (1998) 6024.
[7] T. Kimura, T. Kamata, M. Fuziwara, Y. Takano, M. Kaneda, Y. Sakamoto, O. Terasaki, Y. Sugahara, K. Kuroda, Angew. Chem. Int. Ed. 39 (2000) 3855.
[8] P. Schmidt-Winkel, W.W. Lukens, D.Y. Zhao, P.D. Yang, B.F. Chmelka, G.D. Stucky, J. Am. Chem. Soc. 121 (1999) 254.
[9] D.Y. Zhao, P.D. Yang, D.I. Margolese, B.F. Chmelka, G.D. Stucky, Chem. Commun. (1998) 2499.
[10] F. Marlow, M.D. McGehee, D.Y. Zhao, B.F. Chmelka, G.D. Stucky, Adv. Mater. 11 (1999) 632.
[11] Q.S. Huo, J.L. Feng, F. Schuth, G.D. Stucky, Chem. Mater. 9 (1997) 14.
[12] N.A. Melosh, P. Lipic, F.S. Bates, F. Wudl, G.D. Stucky, G.H. Fredrickson, B.F. Chmelka, Macromolecules 32 (1999) 4332.
[13] A. Monnier, F. Schuth, Q. Huo, D. Kumar, D. Margolese, R.S. Maxwell, G.D. Stucky, M. Krishnamurty, P. Petroff, A. Firouzi, M. Janicke, B.F. Chmelka, Science 261 (1993) 1299.
[14] D. Zhao, J. Feng, Q. Huo, N. Melosh, G.H. Fredrickson, B.F. Chmelka, G.D. Stucky, Science 279 (1998) 548.
[15] P.T. Tanev, T.J. Pinnavaia, Science 267 (1995) 865.
[16] J. Fan, C. Yu, F. Gao, J. Lei, B. Tian, L. Wang, Q. Luo, B. Tu, W. Zhou, D. Zhao, Angew. Chem. Int. Ed. 42 (2003) 3146.
[17] F. Hoffmann, M. Cornelius, J. Morell, M. Froba, Angew. Chem. Int. Ed. 45 (2006) 3216.
[18] Z. Yang, Y. Lu, Z. Yang, Chem. Commun. (2009) 2270.
[19] C.D. Liang, Z.J. Li, S. Dai, Angew. Chem. Int. Ed. 47 (2008) 3696.
[20] M. Tiemann, Chem. Eur. J. 13 (2007) 8376.
[21] S. Jun, S.H. Joo, R. Ryoo, M. Kruk, M. Jaroniec, Z. Liu, T. Ohsuna, O. Terasaki, J. Am. Chem. Soc. 122 (2000) 10712.
[22] P.Y. Wang, L. Zhao, R. Wu, H. Zhong, H.F. Zou, J. Yang, Q.H. Yang, J. Phys. Chem. C 113 (2009) 1359.
[23] Y. Wan, D. Zhao, Chem. Rev. 107 (2007) 2821.
[24] N. Coen, C. Mothersill, M. Kadhim, E.G. Wright, J. Pathol. 195 (2001) 293.
[25] A. Afkhami, A.R. Zarei, Anal. Sci. 20 (2004) 1711.
[26] S. Goubert-Renaudin, M. Moreau, C. Despas, M. Meyer, F. Denat, B. Lebeau, A. Walcarius, Electroanalysis 21 (2009) 1731.
[27] M. Kim, J. Stripeikis, M. Tudino, Spectrochim. Acta B 64 (2009) 500.
[28] Y.W. Wu, B. Hu, W.L. Hu, Z.C. Jiang, B.Y.Z. Li, J. Hazard. Mater. 42 (2007) 467.
[29] S.R. Yousefi, F. Shemirani, M.R. Jamali, M. Salavati-Niasari, Microchim. Acta 169 (2010) 241.
[30] W.L. Hu, F. Zheng, B. Hu, J. Hazard. Mater. 151 (2008) 58.
[31] M.R. Jamali, Y. Assadi, F. Shemirani, M. Salavati-Niasari, Talanta 71 (2007) 1524.
[32] D. Pérez-Quintanilla, A. Sánchez, I. del Hierro, M. Fajardo, I. Sierra, J. Hazard. Mater. 166 (2009) 1449.
[33] D.n. Pérez-Quintanilla, I. del Hierro, M. Fajardo, I. Sierra, J. Mater. Chem. 16 (2006) 1757.
[34] D.H. Chen, B. Hu, C.Z. Huang, Talanta 78 (2009) 491.
[35] S.R. Yousefi, S.J. Ahmadi, F. Shemirani, M.R. Jamali, M. Salavati-Niasari, Talanta 80 (2009) 212.
[36] C.Z. Huang, B. Hu, Z.C. Jiang, Spectrochim. Acta B 62 (2007) 454.
[37] D.H. Chen, C.Z. Huang, M. He, B. Hu, J. Hazard. Mater. 164 (2009) 1146.
[38] L. Hajiaghababaei, A. Badiei, M.R. Ganjali, S. Heydari, Y. Khaniani, G.M. Ziarani, Desalination 266 (2011) 182.
[39] N.T. Hoai, D.K. Yoo, D. Kim, J. Hazard. Mater. 173 (2010) 462.
[40] H. Peng, J. Wang, Z. Shen, D. Wu, Y. Guan, Analyst 136 (2011) 586.
[41] T.M. Wu, G.R. Wu, H.M. Kao, J.L. Wang, J. Chromatogr. A 1105 (2006) 168.
[42] Y.C. Su, H.M. Kao, J.L. Wang, J. Chromatogr. A 1217 (2010) 5643.
[43] N.R. Neng, A.S. Mestre, A.P. Carvalho, J.M.F. Nogueira, Talanta 83 (2011) 1643.
[44] S.A. Trammell, M. Zeinali, B.J. Melde, P.T. Charles, F.L. Velez, M.A. Dinderman, A. Kusterbeck, M.A. Markowitz, Anal. Chem. 80 (2008) 4627.
[45] B.J. Johnson, B.J. Melde, P.T. Charles, D.C. Cardona, M.A. Dinderman, A.P. Malanoski, S.B. Qadri, Langmuir 24 (2008) 9024.
[46] B.J. Johnson, B.J. Melde, C. Thomas, A.P. Malanoski, I.A. Leska, P.T. Charles, D.A. Parrish, J.R. Deschamps, Sensors 10 (2010) 2315.
[47] R.S. Tirumalai, K.C. Chan, D.A. Prieto, H.J. Issaq, T.P. Conrads, T.D. Veenstra, Mol. Cell. Proteomics 2 (2003) 1096.
[48] C.H. Lee, T.S. Lin, C.Y. Mou, Nano Today 4 (2009) 165.
[49] J. Kim, J. Lee, H.B. Na, B.C. Kim, J.K. Youn, J.H. Kwak, K. Moon, E. Lee, J. Park, A. Dohnalkova, H.G. Park, M.B. Gu, H.N. Chang, J.W. Grate, T. Hyeon, Small 1 (2005) 1203.
[50] D. Goradia, J. Cooney, B.K. Hodnett, E. Magner, J. Mol. Catal. B: Enzym. 32 (2005) 231.
[51] R. Hong, N.O. Fischer, A. Verma, C.M. Goodman, T. Emrick, V.M. Rotello, J. Am. Chem. Soc. 126 (2004) 739.
[52] C.C. You, M. De, V.M. Rotello, Org. Lett. 7 (2005) 5685.
[53] W.Q. Shui, J. Fan, P.Y. Yang, C.L. Liu, J.J. Zhai, J. Lei, Y. Yan, D.Y. Zhao, X. Chen, Anal. Chem. 78 (2006) 4811.

[54] F. Casadonte, L. Pasqua, R. Savino, R. Terracciano, Chem. Eur. J. 16 (2010) 8998.
[55] L. Qiao, Y. Liu, S.P. Hudson, P.Y. Yang, E. Magner, B.H. Liu, Chem. Eur. J. 14 (2008) 151.
[56] C. Zuo, W.J. Yu, X.F. Zhou, D.Y. Zhao, P.Y. Yang, Rapid Commun. Mass Spectrom. 20 (2006) 3139.
[57] Q.H. Min, R.A. Wu, L.A. Zhao, H.Q. Qin, M.L. Ye, J.J. Zhu, H.F. Zou, Chem. Commun. 46 (2010) 6144.
[58] L.D. Fricker, J. Lim, H. Pan, F.Y. Che, Mass Spectrom. Rev. 25 (2006) 327.
[59] M. Soloviev, P. Finch, Proteomics 6 (2006) 744.
[60] R.J. Tian, L.B. Ren, H.J. Ma, X. Li, L.H. Hu, M.L. Ye, R. Wu, Z.J. Tian, Z. Liu, H.F. Zou, J. Chromatogr. A 1216 (2009) 1270.
[61] K. Egeblad, C.H. Christensen, M. Kustova, Chem. Mater. 20 (2008) 946.
[62] H. Tammen, I. Schulte, R. Hess, C. Menzel, M. Kellmann, T. Mohring, P. Schulz-Knappe, Proteomics 5 (2005) 3414.
[63] J. Villanueva, J. Philip, D. Entenberg, C.A. Chaparro, M.K. Tanwar, E.C. Holland, P. Tempst, Anal. Chem. 76 (2004) 1560.
[64] S. Camerini, M.L. Polci, L.A. Liotta, E.F. Petricoin, W. Zhou, Proteomics Clin. Appl. 1 (2007) 176.
[65] O. Chertov, A. Biragyn, L.W. Kwak, J.T. Simpson, T. Boronina, V.M. Hoang, D.A. Prieto, T.P. Conrads, T.D. Veenstra, R.J. Fisher, Proteomics 4 (2004) 1195.
[66] P. Roy, T. Dey, K. Lee, D. Kim, B. Fabry, P. Schmuki, J. Am. Chem. Soc. 132 (2010) 7893.
[67] J.J. Wan, K. Qian, J. Zhang, F. Liu, Y.H. Wang, P.Y. Yang, B.H. Liu, C.Z. Yu, Langmuir 26 (2010) 7444.
[68] Y. Hu, A. Bouamrani, E. Tasciotti, L. Li, X.W. Liu, M. Ferrari, ACS Nano 4 (2010) 439.
[69] H.M. Chen, S.S. Liu, H.L. Yang, Y. Mao, C.H. Deng, X.M. Zhang, P.Y. Yang, Proteomics 10 (2010) 930.
[70] S.S. Liu, H.M. Chen, X.H. Lu, C.H. Deng, X.M. Zhang, P.Y. Yang, Angew. Chem. Int. Ed. 49 (2010) 7557.
[71] S.F. Yu, S.B. Lee, M. Kang, C.R. Martin, Nano Lett. 1 (2001) 495.
[72] M. Zhang, Y.P. Wu, X.Z. Feng, X.W. He, L.X. Chen, Y.K. Zhang, J. Mater. Chem. 20 (2010) 5835.
[73] X.S. Peng, J. Jin, I. Ichinose, Adv. Funct. Mater. 17 (2007) 1849.
[74] L. Zhang, S.Z. Qiao, Y.G. Jin, H.G. Yang, S. Budihartono, F. Stahr, Z.F. Yan, X.L. Wang, Z.P. Hao, G.Q. Lu, Adv. Funct. Mater. 18 (2008) 3203.
[75] L. Qin, X.W. He, W. Zhang, W.Y. Li, Y.K. Zhang, J. Chromatogr. A 1216 (2009) 807.
[76] T. Hunter, Cell 100 (2000) 113.
[77] M. Mann, O.N. Jensen, Nat. Biotechnol. 21 (2003) 255.
[78] H. Jumaa, R.W. Hendriks, M. Reth, Annu. Rev. Immunol. 23 (2005) 415.
[79] P.H. Huang, F.M. White, Mol. Cell 31 (2008) 777.
[80] D.T. McLachlin, B.T. Chait, Curr. Opin. Chem. Biol. 5 (2001) 591.
[81] M.R. Larsen, T.E. Thingholm, O.N. Jensen, P. Roepstorff, T.J. Jorgensen, Mol. Cell. Proteomics 4 (2005) 873.
[82] H. Zhou, R. Tian, M. Ye, S. Xu, S. Feng, C. Pan, X. Jiang, X. Li, H. Zou, Electrophoresis 28 (2007) 2201.
[83] L. Han, Z. Shan, D.H. Chen, X.J. Yu, P.Y. Yang, B. Tu, D.Y. Zhao, J. Colloid Interface Sci. 318 (2008) 315.
[84] C. Pan, M. Ye, Y. Liu, S. Feng, X. Jiang, G. Han, J. Zhu, H. Zou, J. Proteome Res. 5 (2006) 3114.
[85] M.C. Posewitz, P. Tempst, Anal. Chem. 71 (1999) 2883.
[86] J. Tang, P. Yin, X.H. Lu, D.W. Qi, Y. Mao, C.H. Deng, P.Y. Yang, X.M. Zhang, J. Chromatogr. A 1217 (2010) 2197.
[87] Z. Lu, J. Duan, L. He, Y. Hu, Y. Yin, Anal. Chem. 82 (2010) 7249.
[88] C.A. Nelson, J.R. Szczech, Q.G. Xu, M.J. Lawrence, S. Jin, Y. Ge, Chem. Commun. (2009) 6607.
[89] C.A. Nelson, J.R. Szczech, C.J. Dooley, Q. Xu, M.J. Lawrence, H. Zhu, S. Jin, Y. Ge, Anal. Chem. 82 (2010) 7193.
[90] H.H. Wan, J.Y. Yan, L. Yu, X.L. Zhang, X.Y. Xue, X.L. Li, X.M. Liang, Talanta 82 (2010) 1701.
[91] J.H. Wu, X.S. Li, Y. Zhao, Q.A. Gao, L. Guo, Y.Q. Feng, Chem. Commun. 46 (2010) 9031.
[92] A. Eriksson, J. Bergquist, K. Edwards, A. Hagfeldt, D. Malmstrom, V. Agmo Hernandez, Anal. Chem. 82 (2010) 4577.
[93] A. Eriksson, J. Bergquist, K. Edwards, A. Hagfeldt, D. Malmstrom, V.A. Hernandez, Anal. Chem. 83 (2011) 761.
[94] G. Cheng, J.-L. Zhang, Y.-L. Liu, D.-H. Sun, J.-Z. Ni, Chem. Commun. 47 (2011) 5732.
[95] Y. Zhang, C. Chen, H.Q. Qin, R.A. Wu, H.F. Zou, Chem. Commun. 46 (2010) 2271.
[96] L. Hu, H. Zhou, Y. Li, S. Sun, L. Guo, M. Ye, X. Tian, J. Gu, S. Yang, H. Zou, Anal. Chem. 81 (2009) 94.
[97] Z.D. Lu, M.M. Ye, N. Li, W.W. Zhong, Y.D. Yin, Angew. Chem. Int. Ed. 49 (2010) 1862.
[98] L. Lehle, S. Strahl, W. Tanner, Angew. Chem. Int. Ed. 45 (2006) 6802.
[99] J. Hirabayashi, Glycoconj. J. 21 (2004) 35.
[100] Y. Wada, M. Tajiri, S. Yoshida, Anal. Chem. 76 (2004) 6560.
[101] Y. Tian, Y. Zhou, S. Elliott, R. Aebersold, H. Zhang, Nat. Protoc. 2 (2007) 334.
[102] Y.W. Xu, Z.X. Wu, L.J. Zhang, H.J. Lu, P.Y. Yang, P.A. Webley, D.Y. Zhao, Anal. Chem. 81 (2009) 503.